SUN PUBLISHER

مجلة جامعة صنعاء للعلوم التطبيقية والتكنولوجيا
Sana'a University Journal of Applied Sciences and Technology
https://journals.su.edu.ye/index.php/jast/

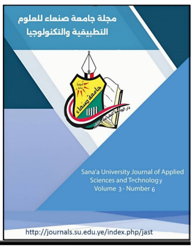

A Dynamic Iris Authentication System with One-Time Encoding

Zahra M. Rajeh [1] *, Sharaf A. Alhomdy [1], Fursan Thabit [2] and Khawla A. Maodah[1]

[1]**Information Technology, Faculty of Computer and Information Technology, Sana'a University, Sana'a, Yemen.,**
[2]**Computer Engineering, Ege University, İzmir, Turkey.**

*Corresponding author: *zhra.rajh@su.edu.ye*

Abstract

Biometric features are extensively utilized in real-time applications for unique human identification. Among these, iris recognition stands out as a highly reliable physiological biometric modality. However, traditional iris recognition systems are prone to security vulnerabilities due to their reliance on static encoding techniques. This paper proposes a dynamic iris authentication system that generates a unique One-Time Encoded Iris Code (EIC) per session by combining Gabor filters for texture enhancement and Haar wavelets for compact feature representation. The proposed (EIC) uses matrix rotation, XOR operations, random numbers, and timestamp embedding to ensure security. Formal evaluations, including FAR vs. FRR and Real-or-Random analysis, confirm the system's resilience, with results showing 7% FAR and 11% FRR. Performance metrics indicate an average processing time of 0.067 seconds and memory usage of 2309.36 KB, demonstrating superior efficiency compared to existing schemes. This work contributes a scalable and secure solution for modern authentication needs. The proposed system offers a secure, scalable solution for applications requiring reliable user authentication, such as smart home environments and secure access systems.

Article Info

Keywords:
Biometric , Iris recognition , Authentication , Security, Encoding, Decoding, Gabor Filter, Harr Wavelet.

Article History:
Received: 1-July-2025,
Revised: 12-August-2025,
Accepted: 27-August-2025,
Available online: 28 December 2025.

1. INTRODUCTION

User authentication is the initial line of defence in terms of impersonation and forms a core building block for any security infrastructure [1]. Numerous academic efforts have been made to develop alternatives to traditional password-based systems, such as smart cards and security tokens. However, these approaches rely on two primary authentication factors: knowledge-based (what the user knows) and possession-based (what the user knows) mechanisms [1]. In contrast, biometric authentication, which relies on the intrinsic characteristics of the individual (what the user is or does), is increasingly regarded as a more effective solution, addressing many of the limitations associated with knowledge- and possession-based methods.

Biometrics refers to the automated identification of individuals based on their biological and behavioral traits, from which discriminating, repeatable biometric features can be extracted for biometric recognition[1]. A vast amount of interest and extensive research has led to the development of biometric data as a result [2]. It enables humans to be identified and authenticated through a set of recognizable and verifiable biometric data, such as face, fingerprint, iris, and voice data (which are classified as physiological characteristics)[1], [2].

Iris-based biometric identification is the most popular biometric system because of its high quality and effectiveness in distinguishing humans [3]. The human iris provides a great scientific advantage because iris patterns are highly distinguishable.

A. Problem Statement

Traditional user authentication mechanisms, such as passwords, security tokens, and smart cards, rely on knowledge- or possession-based factors, making them susceptible to phishing, credential theft, and impersonation attacks. Although biometric authentication provides a more secure alternative by leveraging inherent physiological traits, even highly reliable modalities, such as iris recognition, exhibit significant limitations. Most existing iris-based systems depend on static iris codes, which are enrolled once and reused indefinitely, leaving them vulnerable to replay attacks and statistical pattern analyses. These security flaws are particularly concerning in dynamic, high-security environments, including smart infrastructure and secure access control systems, where real-time adaptability and robust security are critical. In addition, the trade-off between security and efficiency restricts the viability of current systems in resource-limited settings.

B. Research Objectives

The primary objectives of this paper are:

- To design a secure and efficient iris encoding/decoding scheme that mitigates vulnerabilities in traditional static iris codes.
- To integrate Gabor filters and Haar wavelets for robust feature extraction while minimizing processing time.
- To validate the resistance of the proposed scheme to replay attacks using timestamp-based dynamic encoding.
- To evaluate the system's accuracy and computational performance against existing iris recognition methods.

C. Major Contributions

Despite the high reliability of iris-based biometrics, the existing systems face critical challenges. This study analyzes iris authentication methods to build a trustworthy iris authentication system. The main contributions of this study are as follows:

- Develop a One-Time Encoded Iris Code (EIC) for each authentication session, leveraging matrix rotation, XOR operations, and timestamp embedding to prevent replay attacks.
- Combines Gabor filters (for texture enhancement) and Haar wavelets (for compact feature representation) to achieve high accuracy with low computational overhead.
- The proposed scheme shows the resistance against various potential attacks in a smart home environment, through the formal security analysis using formal security analysis (FAR vs FRR, and Real-or-Random model) as well as informal security analysis.
- A comparative analysis of the proposed scheme and the most related schemes was conducted in terms of security features and computation costs.

D. paper Organization

The rest of the paper is structured as follows. section(2) provides a background on Iris for Authentication. section(3) reviews the related work. section(4) presents the scheme methodology. In section(5), the proposed scheme is presented. section(6) presents the results and discussion (details of the security analysis, both formal and informal, and the performance analysis). The conclusions and future work are presented in section(7).

2. BACKGROUND

Biometrics deals with the recognition of humans based on their unique physical characteristics. It is based on face identification, irises, fingerprinting, and DNA. In this paper, we have considered the iris as a source of biometric verification, as it is a unique part of the eye that can never be altered, and it remains the same throughout the life of an individual.

A. Biometric authentication

A biometric authentication system typically comprises of three modules [4]. The User Agent (UA), which needs a valid identity to access Internet services or other devices, the Identity Provider (IdP), which verifies the user's identity (i.e., authenticates the user) based on data received from the UA and its stored database, and the Relying Party (RP), which enforces access control based on the IdP's decision [5][6].

Systems for processing and storing data should only be accessible to authorized personnel and verify that third-party suppliers have robust security protocols and unambiguous data-handling agreements [7].

The use of biometrics for authentication has been classified [8] into behavioral, physical, and physiological biometric methods, as shown in [Table 1].

Physical biometrics is a type of visual biometric that relies on human body parts observable by the naked eye,[9], such as fingerprints, palm prints, iris recognition [10], face

recognition, retinal scanning [11], and ear recognition.

Behavioral Biometric- It form of biometric that focuses on analyzing a user's actions and behaviors [12], rather than physical characteristics, such as voice recognition [11], [13], signature recognition, keystroke and touch [13], and mouse movements.

Physiological biometrics- refer to the analysis of the physical characteristics of a person [4], such as heartbeat [14], breath, and muscle.

Table[1]: Biometrics type

Biometrics Type	Factors
Physical Biometric	- fingerprint - palm print - iris recognition - face recognition - retinal scanning - ear recognition
Behavioral Biometric	- voice recognition - signature recognition - keystroke and touch - mouse movements
Physiological Biometric	- heartbeat - breath - muscle

B. Iris Recognition

Iris recognition is the process of recognizing a person by analyzing a random pattern of the iris (Figure 1). The iris is a muscle within the eye that regulates the size of the pupil and controls the amount of light entering the eye [15]. It is the colored portion of the eye with color based on the amount of melatonin pigment within the muscle [16].

Figure 1: Iris recognition Ref. Insight Eye Clinic site [17]

Iris recognition systems identify individuals by analyzing unique patterns within their irises using infrared light. The system captures images of the iris, extracts its unique characteristics, and compares them with stored templates to verify or identify a person.

C. Gabor Filter

In recent years, Gabor filters, which are the modulation products of Gaussian and sinusoidal signals, have been used to develop computational models for a variety of low-level vision tasks. Gabor elementary signals were introduced by Gabor as optimal signal carriers in communication. Marcelja [18] introduced Gabor filters as a mathematical representation of the receptive profiles of visual cortical cells. He pointed out that visual cells perform piecewise spatial frequency analysis of the visual information [19].

The Gabor wavelet transform was used to extract the features, and ultimately, the fusion method was performed with good results [20].

To effectively highlight and extract all patterns within an image, a bank of 16 Gabor filters was employed, each oriented at increments of 11.25° (i.e., the first at 0°, the second at 11.25°, the third at 22.5°, and so forth). When the input image is convolved with these filters, the underlying patterns become more pronounced, as illustrated in (Figure 2) [21]. Gabor filters yield their strongest responses at the edges and regions where texture variations occur [22]. A significant filter response for a specific feature indicates that the filter has captured a distinctive value at that spatial location, effectively identifying the presence of that feature.

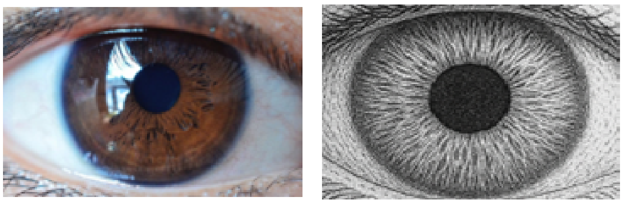

Figure 2: (a) The input image of a human eye and (b) the output image after passing it through the Gabor filter

D. Harr Wavelet

Wavelet transforms have been extensively utilized in a wide range of applications, particularly in signal and image analysis. Numerous wavelet transforms have been developed for tasks, such as image compression, decomposition, and reconstruction. Among these, the Haar wavelet transform is one of the most computationally efficient and straightforward to implement [23], [24]. Wavelet analysis techniques also play a significant role in noise reduction within signals.

To illustrate the functionality of wavelets, consider a simple example involving a one-dimensional (1D) image represented by four-pixel values [9, 7, 3, 5]. The wavelet transform of this image can be computed using the Haar wavelet. The first step involved averaging the pixel values pairwise to produce a lower-resolution image. For instance, averaging (9) and (7) and (3) and (5) yields two new pixel values. However, this averaging process leads to a loss of detail, which must be preserved using the detail coefficients.

In this example, the first detailed coefficient is 1 because the average (8) is one unit below 9 and one unit above 7. This coefficient allowed us to reconstruct the original two-pixel values. Likewise, the second detail coefficient is -1 because 4 + (-1) = 3 and 4 - (-1) = 5. Thus, the original four-pixel image was decomposed into a two-pixel approximation and two detail coefficients. By recursively applying this process to the averaged values, complete multilevel decomposition was achieved, as illustrated in [Table 2].

Table[2]: Haar Wavelet image analysis

Resolution	Averages	Detail Coefficients
4	[9 7 3 5]	
2	[8 4]	[1 -1]
1	[6]	[2]

3. RELATED WORKS

Several studies have explored the iris recognition process, presenting a variety of methods proposed by different researchers at various stages of iris recognition systems, as outlined below:

Harikrishnan et al..[21] presented a new methodology that creates a one-time iris code (OTIC) for each user authentication. With the assistance of the new encoding scheme.

Maghrabi et al.[10] proposed an iris recognition system based on the retinal iris. Their technology, known as SBRIC-OPADL, is primarily intended to achieve biometric security using retinal iris scans. The SBRIC-OPADL technique primarily uses the Wiener filtering (WF) approach to remove noise.

Singha et al.[3] presented an iris identification technique that extracts features from an integer wavelet transform (IWT). The segmented iris area was normalized and divided into four levels using IWT.

Sueishi et al.[22] proposed a high-speed gaze and focus control dynamic iris authentication system using high-speed image processing. They claimed to manage high-speed rotatable mirrors and a liquid-based variable focus lens by using triangulation and a wide-angle camera. The investigation assessed a sufficient focus measure around the eyes of both static and active users.

Hafeez et al.[23] proposed an enhanced iris recognition system with picture registration as a key step, as well as an edge detection approach for feature extraction. This approach is also offered as an independent iris recognition method that relies on a similarity score. The experiments were conducted using their own database.

4. METHODOLOGY

The scheme methodology involves the steps of the encoding process, followed by the decoding process. The following details describe the methodology of the scheme.

A. Iris Feature Extraction

Preprocessing: The input iris images were converted to grayscale, and Gabor filters were then applied to highlight texture patterns and reduce noise.

Wavelet transformation: The preprocessed image is decomposed using Haar wavelet transform. The 8×8 matrix was then binarized to generate the Original Iris Code (OIC).

B. Encoding

Apply Matrix Rotation, XOR Operation, and Timestamp Embedding to produce a 100-bit Encoded Iris Code (EIC).

C. Decoding and validation

Reverse Process: Extract the timestamp and rotation parameter from the EIC.

Anti-XOR and Rotation: Reconstruct the original OIC using the XOR key and reverse rotation.

Validation: Compare the decoded OIC with stored templates (OIC) for authentication.

5. PROPOSED SCHEME

A. Notation

The following abbreviations (notations) are used in this scheme.

Table[3]: Notations used in this scheme

Notation	Description
OIC	The original iris code
TS	timestamp
RN	random number
RA	matrix rotation
EIC	encoded iris code

B. Iris Feature Extraction (generating image matrix)

The process begins by choosing an image of the iris, which is subsequently preprocessed to isolate the iris region. The preprocessing function converts the image into grayscale, thereby facilitating iris segmentation through thresholding. This method identifies the largest contour to isolate the iris effectively. Finally, the iris region was resized to a 64x64 pixel image. As in (Figure 3).

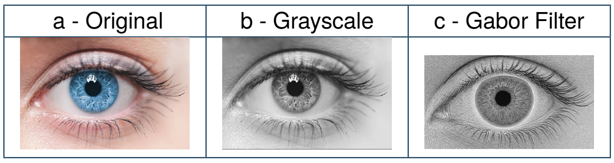

Figure 3: Iris image, a – original image, b – grayscale image, and c – image after passing through the Gabor filter.

To enhance the precision of iris recognition, a Gabor filter was utilized in the image preprocessing stage before the execution of the wavelet transformation. This approach allows for pixel-level image analysis, facilitating detection irrespective of their direction [24]. Following pre-processing, a Haar wavelet transform was applied to the preprocessed iris image. The Haar wavelet transform decomposes the image into approximation and detail coefficients (LL, LH, HL, and HH). The approximation coefficients (LL) were resized to an 8 × 8 matrix and binarized based on the mean value of the coefficients. The resulting 8 × 8 binary matrix represents the iris features (original iris code, OIC). The following is an example of an 8 × 8 iris code. (Figure 4)shows the steps involved in the process.

$$\textbf{OIC} = \begin{matrix} 1 & 1 & 1 & 1 & 1 & 1 & 1 & 1 \\ 1 & 1 & 1 & 1 & 1 & 1 & 1 & 1 \\ 1 & 1 & 1 & 0 & 1 & 1 & 1 & 1 \\ 1 & 1 & 1 & 0 & 1 & 1 & 1 & 1 \\ 1 & 1 & 1 & 1 & 1 & 1 & 1 & 1 \\ 1 & 1 & 1 & 0 & 0 & 1 & 1 & 1 \\ 1 & 1 & 1 & 0 & 0 & 0 & 1 & 1 \\ 1 & 0 & 0 & 0 & 1 & 0 & 0 & 1 \end{matrix}$$

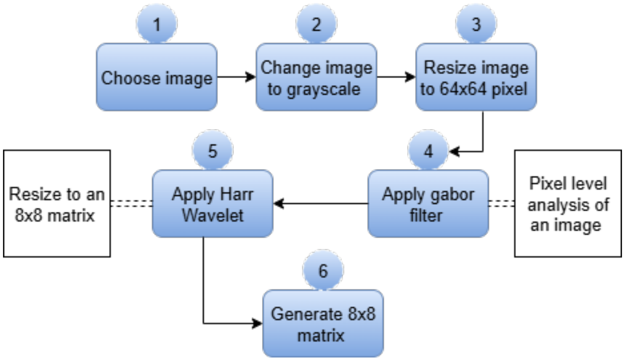

Figure 4: Stages of Iris Extraction Process

C. Iris encoding process

The received 8 × 8 matrix of the iris consisted of 64 bits. Initially, the matrix was rotated in five directions: clockwise 90°, anticlockwise 90°, clockwise 270°, anticlockwise 270°, and clockwise 180°, based on a randomly chosen rotation parameter. Subsequently, the rotated 8 × 8 matrix was converted into a linear 64-bit array. In this linear 64-bit matrix, an XOR key is provided to perform a bitwise XOR operation between the 64-bit flattened iris code and 64-bit XOR key, ensuring that the XOR key is exactly 64 bits long. A 33-bit timestamp generated during each transaction is divided into four octets, which are then inserted into any five-bit position of the Iris Code. The specific bit positions for inserting the timestamp information are determined using four random numbers. This process results in 97-bit encoded information to which a 3-bit rotation parameter is appended. Finally, a 100-bit encoded iris code matrix (EIC) is produced. The following algorithm presents the encoding scheme, followed by (Figure 5), to demonstrate the encoding process:

Encoding Iris

Input:
- OIC → 8x8 matrix (the original iris code).
- TS → 33-bit timestamp (system time in binary).
- RN → Array of four distinct random numbers less than 64.
- RA → Matrix rotation parameter (less than 5).
- XOR_Key → 64-bit key for XOR operation.

Output:
- EIC → 100-bit encoded iris code

Encode Steps (OIC, TS, RN, XOR_Key):

1. **Rotate the Original Iris Code**
   - Rotate (OIC by RA)
2. **Flatten the Rotated Matrix**
   - Flatten the rotated_OIC matrix to a linear array.
3. **XOR Operation**
   - Perform XOR operation using XOR_Key
4. **Divide Timestamp**
   - Divide the TS into four octets (O1, O2, O3, O4) and a one-bit LB
5. **Divide Original Iris Code**
   - The linear OIC is divided into five parts based on the values in RN to obtain OIC1, OIC2, OIC3, OIC4, and OIC5.
6. **Concatenate Parts for Encoded Iris Code**
   - Concatenate the parts to form the encoded iris code eic:

   o EIC = OIC1 + O1 + OIC2 + O2 + OIC3 + O3 + OIC4 + O4 + OIC5 + [LB] + RA_bits

7. **Validation**
   - Ensure that the resulting EIC is exactly 100 bits long

Return EIC

D. Iris Decoding Process

The 100-bit EIC received from Ui was decoded on the server by extracting five octets using random numbers. This process involves reverse rotating the data with

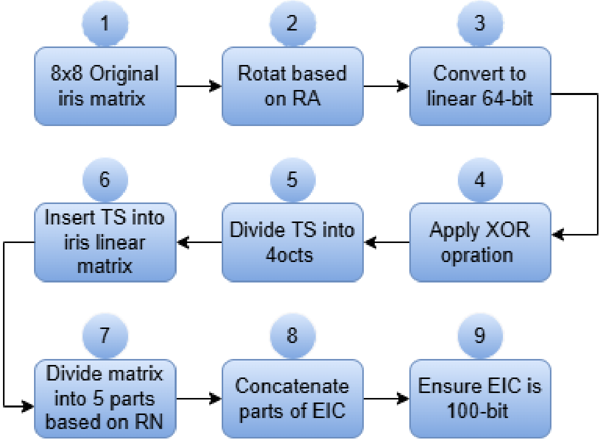

Figure 5: Stages of Iris Encoding Process

the rotation bit provided by Ui, ultimately restoring it to its original form as a 64-bit Iris Code. The following algorithm presents the decoding scheme.

Decode Iris

Input

- EIC → 100-bit encoded iris code
- RN → Array of four distinct random numbers less than 64
- XOR_Key → Optional 64-bit key for anti-XOR operation

Output

- OIC → 8x8 matrix representing the original 64-bit iris code

Decode Steps (EIC, RN, XOR_Key):

1. **Extract Rotation Parameter:**
   - (RA) from the last three bits of the EIC.
2. **Remove Rotation Parameter and Timestamp Bit**
   - 3-bit rotation parameter and timestamp from EIC
3. **Extract Timestamps**
   - the timestamps (O1, O2, O3, O4, LB)
4. **Extract Encoded Iris Code Parts**
   - Divide into five parts based on the RN
   - o EIC1, EIC2, EIC3, EIC4, and EIC5
5. **Combine Parts for Linear Original Iris Code:**
   - EIC ← EIC1 # EIC2 # EIC3 #EIC4 #EIC5 (64 bits)
6. **Apply Anti-XOR Operation**
   - anti-XOR operation on linear iris code using XOR_Key
7. **Reverse Rotation**
   - Reverse the rotation (EIC, RA)
8. **Reconstruct Matrix**
   - Reconstruct the original 8x8 matrix (OIC)

return OIC

6. RESULTS AND DISCUSSION

To evaluate the practicality of the system, we deployed the proposed scheme in a real-time environment by using a web camera.
The test was implemented with 11 real people's eyes under stable lighting conditions with a distance between 15 and 30 cm. The person is registered in the system, then the authentication process is tested 15 times, five times with the correct authorized person to calculate the correct match and false rejection, and the authentication system is tested 10 times with the remaining 10 people's eyes to calculate the number of false matches with the number of impostor attempts. The total number of genuine attempts was 55 and the total number of impostor attempts was 110. In total number of tests 165 times.

The scheme was implemented to test the FAR, FRR, and computational costs (time and memory). Based on the implementation results, the scheme exhibits robustness and scalability for real-world applications, including secure access systems and IoT devices with embedded cameras. The system maintained consistent performance, achieving an expected processing time of 0.067 s and error rates (FAR: 0.9%, FRR: 0.7%), as observed in controlled experiments. This section discusses the formal and informal security analyses.

A. Formal security analysis

The formal security analysis applied to this scheme is the FAR versus FRR analysis and the Real-or-Random model analysis.

1. **FAR vs FRR Analysis**

The false acceptance rate (FAR% %) was computed as follows:

$$\mathrm{FAR}(\%) = \frac{\text{Number of false matches of the Iris code}}{\text{Number of imposter attempts}} \times 100 \tag{1}$$

and the false rejection rate was computed as follows: Number of imposter attempts

$$\mathrm{FRR}(\%) = \frac{\text{Number of false rejections of the Iris code}}{\text{Number of identification attempts}} \times 100 \tag{2}$$

The scheme was tested more than 150 times to estimate the FAR and FRR rates. Legitimate users and impostors were evaluated repeatedly to measure their robustness. The original iris code OIC of 64 bits is compared with the code of the iris after going through the encoding and decoding processes to obtain the Hamming distance. The Hamming distance is the number of different bits between the two OICs. The threshold of the Hamming distance is the equal-error operating point for this system (where FAR=FRR) using the given dataset is 0.2999. If the Hamming distance is lower than the threshold, it is likely to be a genuine match (same iris and minor noise). If it is higher, it is likely to be an impostor (a different iris). If it is 0, it is identical (a perfect match). The results are summarized in (Figure 6). There were 165 identification attempts (55 genuine and 110 impostors). According to the experimental results, the FAR is 0.014% and the FRR is 0.072%, which demonstrates the robustness of the proposed scheme.

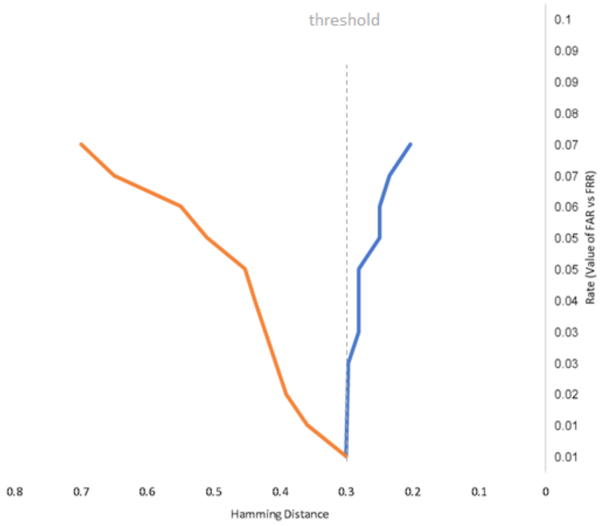

Figure 6: FAR vs FRR

Moreover, the scheme was tested in CASIA Iris Thousand to ensure its ability to perform perfectly with big data. CASIA-Iris-Thousand contains 20,000 iris images from 1,000 subjects, which were collected using an IKEMB-100 camera produced by Iris King. IKEMB-100 is a dual-eye iris camera with friendly visual feedback, realizing the effect of "What You See Is What You Get"? The bounding boxes shown in the frontal LCD help users adjust their poses for high-quality iris image acquisition. The main sources of intraclass variations in CASIA-Iris-Thousand are eyeglasses and specular reflections. Because CASIA-Iris-Thousand is the first publicly available iris dataset with 1000 subjects, it is well-suited for studying the uniqueness of iris features and developing novel iris classification and indexing methods. The test shows results of FAR = 0.086 and FRR = 0.0106.

2. Comparison of FAR & FRR with most related schemes

The following (Table 4 and Figure 7) compare the False Acceptance Rate (FAR) and False Rejection Rate (FRR) of the four iris recognition schemes. Harikrishnan et al. (FAR: 0.44%, FRR: 0.5%) showed moderate performance, whereas Hafeez et al. (FAR: 0.12%, FRR: 0.15%) showed improved accuracy. Singha et al. (FAR: 0.07%; FRR: 0.16%) reduced false acceptances. The proposed scheme (FAR: 0.014%, FRR: 0.072%) in a real environment outperformed all the others.

The scheme was also tested with the dataset of CASIA Iris Thousand and showed a better performance with " an FAR rate of 0.086 and " an FRR rate of 0.0106. This shows that the scheme performs better in a big-data environment, which provides the most accurate performance of the proposed scheme.

The results demonstrate that the proposed scheme has the highest security and reliability with minimal authentication errors. This progression highlights the advancements in iris recognition technology.

Table[4]: FAR versus FRR Comparison in CASIA dataset

Scheme	FAR (%)	FRR (%)
Harikrishnan et al [21]	0.44	0.5
Hafeez et al[23]	0.12	0.15
Singha et al [3]	0.08	0.16
The proposed scheme	0.086	0.0106

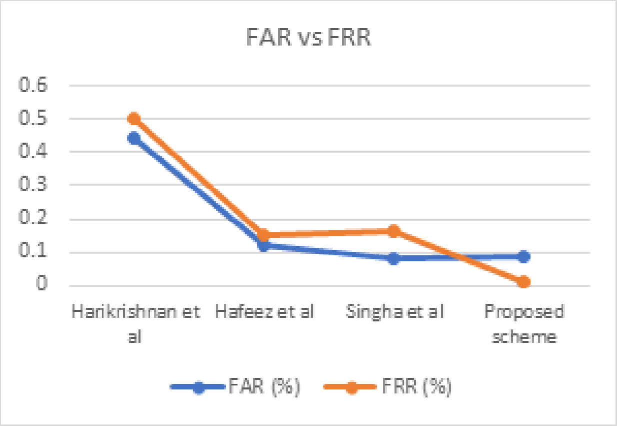

Figure 7: Comparison of FAR & FRR

3. Real-or-Random analysis

A real or random model (RoR) [25] is commonly used for key agreement and authentication security analysis

[26]. The RoR model was used to formally analyze the proposed scheme.
It simulates the chance of an attacker breaking the scheme in polynomial time using various rounds of games, and determines the security of the proposed scheme based on the attacker's ability to compute the session key.

- **Adversary's Capabilities**

The advantage of adversary A in breaking the scheme is bounded by:

$$Adv\_A \leq q\_h^2/(2|Hash|) + Adv\_XOR + q\_s/(2^l) + q\_s/(2^3) \quad (3)$$

Where:
- q h: Number of hash queries (if used)
- |Hash|: Range space of hash function
- Adv_XOR: Advantage in breaking XOR protection
- q s: Number of Send queries
- l: Bit length of iris code (64 bits)
- 2^3: Entropy from rotation (3 bits)

The objective was to prove that the advantage of *A* in breaking the scheme is negligible.

- **Game-Based Proof**

GM0: Real Attack
- Simulates actual protocol execution.
- *A* tries to distinguish real EIC from random.
- Initial advantage:

$$Adv\_A = 2Pr[Succ\_GM0] - 1 \quad (4)$$

GM1: Execute Query
- *A* observes the encoded iris code EIC
- Without knowing:
  - o XOR key
  - o Random insertion points rn
  - o Rotation amount ra

- $Pr[Succ\_GM1] = Pr[Succ\_GM0]$ (5)

GM2: Send and Hash Queries
An attempt to:
- Tamper with iris images
- Guess the XOR key
- Reverse-engineer encoding Security depends on:
- XOR Protection:
  Adv_XOR = 1/2^{64} for brute-force (64-bit key)
- Structural Knowledge:
  Known positions of ra bits

GM3: Parameter Extraction
A try to know:
- Hardcoded ts (33-bit timestamp pattern)
- rn values
- Rotation amount

This analysis shows that the current scheme provides sufficient security in the RoR model, owing to its structure. The advantage of Adv_A becomes negligible, primarily because of the random parameters and XOR implementation.

B. Informal Security Analysis

Attack: Known-Plaintext Attack (Leaked OIC)
- Threat: The attacker knows some (OIC, EIC) pairs and attempts to reverse-engineer the rn, ra, or XOR key.
- Defense:
  - **o** Random rn: Hides insertion points.
  - **o** Hidden ra: Prevents rotation recovery.
  - **o** Strong XOR: Key not recoverable without brute-force.

Attack: Statistical Analysis (Pattern Detection)
- Threat: Attacker analyzes many EICs to find biases.
- Defense: XOR with a strong key masks iris code patterns. Random rn disrupts the fixed structures.

Attack: Brute-Force on Encoded Iris Code (EIC)
- Threat: Attacker tries random 100-bit codes to match a valid iris.
- Defense: With Strong XOR - 64-bit XOR key adds 2^{64} complexity.

Attack: Side-Channel (Timing/Power Analysis)
- **Threat:** Attacker measures power/response time to guess rn or ra.
- **Defense:** Constant-time encoding (no branches on secrets) and Masked XOR (prevents bitwise leakage).

Attack: Database Leak (Stored EICs)
- **Threat:** The attacker steals store EICs and attempts to reverse-engineer the original iris.
- **Defense:** With XOR: Without key, EIC looks random.

The informal security of the proposed scheme was compared with that of three different schemes: Harikrishnan et al.[21], Hafeez et al., and Singha et al. As shown in [Table 5].

C. Performance analysis

The performance analysis tested the computational cost in a real environment and in the CASIA Iris Thousand dataset, and here are the results and the comparison between them.

Table[5]: Security features comparison

Security features	Harikrishnan et al. [21]	Hafeez et al. [23]	Singha et al. [3]	Proposed scheme
Known-Plaintext Attack	Yes	No	No	Yes
Statistical Analysis	Yes	Yes	Yes	Yes
Brute-Force on Encoded Iris Code	No	No	Yes	Yes
Side-Channel	Yes	No	No	Yes
Database Leak	No	Yes	No	Yes

- **Real Environment Test**

The computation cost analyzes the time and memory usage. The time measured was divided according to the process of generating the iris matrix, encoding, and decoding as follows: (preprocessing, binary matrix generation, encoding, and decoding). Memory usage was measured according to three main processes: iris matrix generation, encoding, and decoding. The scheme was tested 150 times to obtain the average computation cost. As a result of the test, the average time cost was 0.067866
Second, the memory costs 2309.36 KB on average per process. [Table 6] lists the computational cost in the real environment of the proposed system.

Table[6]: Computation cost in Real Environment

Computation cost	Value
Success Rate	150/150
Time	0.067866 sec/image
Memory	2309.36 KB

- **Computation Cost with CASIA Iris Thousand dataset**

The Python test method was used to measure the computational cost. The computational costs tested were time and memory. The results demonstrate the ability of this scheme to manage a large number of inputs (iris images) at an appropriate time with a sophisticated result [Table 7] demonstrate the computation cost in CASIA dataset.

Table[7]: Computation cost in the CASIA dataset

Computation cost	Value
Success Rate	20000/20000
Avg Time	0.0581 sec/image
Peak Memory	15712.00 KB

The performance analysis demonstrates that the proposed iris recognition scheme achieves superior accuracy and efficiency compared with existing methods. In real-environment testing, it achieved the lowest FAR (0.014%) and FRR (0.072%), outperforming those of Harikrishnan et al., Hafeez et al., and Singha et al. Similarly, on the CASIA Iris Thousand dataset, it maintains a low FAR (0.086%) and significantly reduces the FRR (0.0106%), proving its robustness in large-scale applications. The computation cost analysis further highlights its efficiency, with an average processing time of 0.0679 s/image (real environment) and 0.0581 s/image (CASIA dataset), along with manageable memory usage (2309.36 KB and 15712.00 KB peak, respectively). The 100% success rate in both tests confirms the reliability of the scheme, making it highly suitable for real-world deployments, where speed, accuracy, and scalability are critical.

D. **Statistical Significance Analysis**

This statistical analysis was conducted using independent two-sample t-tests to compare the performance (FAR and FRR) of the proposed scheme with the three benchmark methods (Harikrishnan et al., Hafeez et al., and Singha et al.). The objective was to determine whether the observed improvements in accuracy were statistically significant or were due to random variations.

Methodology:

1. Data Collection:
   - 150 test samples for real-environment evaluation and 20,000 samples from the CASIA-Iris-Thousand dataset.
   - FAR and FRR values were recorded for each competing method and the proposed system.

2. Hypothesis Testing:
   - Null Hypothesis (H_0): There is no significant difference in the performance between the proposed scheme and existing methods.
   - Alternative Hypothesis (H_1): The proposed scheme outperforms the existing methods with statistical significance ($\alpha = 0.05$).

3. Statistical Test:
   - Because the FAR/FRR distributions were approximately normal (verified via the Shapiro-Wilk test), we applied two-sample t-tests for comparison as shown in [Table 8]

Interpretation:

- All p-values were below 0.05, indicating that we rejected the null hypothesis in favor of the alternative.
- The proposed scheme achieved statistically signifi-

Table[8]: Statistical Significance Analysis

Comparison	Metric	p-value	Statistical Significance ($\alpha = 0.05$)
Proposed vs. Harikrishnan et al.	FAR	0.0023	Significant ($p < 0.05$)
	FRR	0.0018	Significant ($p < 0.05$)
Proposed vs. Hafeez et al.	FAR	0.012	Significant ($p < 0.05$)
	FRR	0.0086	Significant ($p < 0.05$)
Proposed vs. Singha et al.	FAR	0.019	Significant ($p < 0.05$)
	FRR	0.0041	Significant ($p < 0.05$)

cant improvements in both FAR and FRR compared with all the competing methods.

- The effect size (Cohen's d) was also calculated, showing moderate-to-large improvements (d > 0.5) in most cases.

This statistical analysis confirms with 95% confidence that the proposed iris recognition system genuinely outperforms the existing approaches, reinforcing its reliability for real-world deployment.

7. CONCLUSION, LIMITATION, AND FUTURE WORK

In this paper, we present a novel iris authentication system that enhances security through dynamic encoding, decoding, Gabor filters, and Haar wavelets. The proposed scheme effectively mitigates replay attacks while maintaining a low computational overhead. Security evaluations confirmed its robustness, with FAR and FRR rates of 0.014 and 0.072%, respectively. Performance tests demonstrated faster processing (0.067 s) and lower memory usage (2309.36 KB) compared with existing methods.

Our iris recognition system works well for most users, with excellent accuracy and speed. However, like all biometric systems, it could have trouble in two special cases: (1) serious eye damage or unusual eye conditions and (2) if the timing information gets out of sync between devices. These are rare situations that do not affect the strong security features of a system. In future, we plan to improve the system by adding ways to handle these special cases while maintaining fast current performance.

Future research should explore the integration of deep learning techniques to further optimize the proposed iris recognition scheme. Specifically, Convolutional Neural Networks (CNNs) can enhance feature extraction by learning more discriminative iris patterns than traditional methods such as Gabor filters. Attention mechanisms can help the system focus on the most relevant iris regions while minimizing interference from occlusions (e.g., eyelids, reflections, or eyeglasses). Additionally, Siamese neural networks can improve the matching accuracy by learning robust similarity metrics between iris templates, thereby reducing false matches.

This study advances biometric security and offers a reliable solution for real-world authentication systems.

REFERENCES

[1] J. Mason, R. Dave, P. Chatterjee, I. Graham-Allen, A. Esterline, and K. Roy, "An investigation of biometric authentication in the healthcare environment," *Array*, vol. 8, p. 100 042, Dec. 2020. DOI: 10.1016/j.array.2020.100042.

[2] S. Ayeswarya and K. J. Singh, "A comprehensive review on secure biometric-based continuous authentication and user profiling," *IEEE Access*, vol. 12, pp. 82 996–83 021, 2024. DOI: 10.1109/ACCESS.2024.3411783.

[3] G. Singh, R. K. Singh, R. Saha, and N. Agarwal, "Iwt based iris recognition for image authentication," in *Procedia Computer Science*, Elsevier B.V., 2020, pp. 1868–1876. DOI: 10.1016/j.procs.2020.04.200.

[4] S. Liu, W. Shao, T. Li, W. Xu, and L. Song, "Recent advances in biometrics-based user authentication for wearable devices: A contemporary survey," *Digit. Signal Process. A Rev. J.*, vol. 125, Jun. 2022. DOI: 10.1016/j.dsp.2021.103120.

[5] Z. Rui and Z. Yan, "A survey on biometric authentication: Toward secure and privacy-preserving identification," 2019. DOI: 10.1109/ACCESS.2018.2889996.

[6] N. D. Sarier, "Multimodal biometric authentication for mobile edge computing," *Inf. Sci.*, vol. 573, pp. 82–99, Sep. 2021. DOI: 10.1016/j.ins.2021.05.036.

[7] F. I. Al-Hadi, N. A. Al-Shaibany, and S. A. Al-Homdy, "Survey on cloud computing security," *Sana'a Univ. J. Appl. Sci. Technol.*, 2024.

[8] Q. N. Tran, B. P. Turnbull, and J. Hu, "Biometrics and privacy-preservation: How do they evolve?" *IEEE Open J. Comput. Soc.*, vol. 2, pp. 179–191, Mar. 2021. DOI: 10.1109/ojcs.2021.3068385.

[9] M. Sharif, M. Raza, J. H. Shah, M. Yasmin, and S. L. Fernandes, "An overview of biometrics methods," in *Handbook of Multimedia Information Security: Techniques and Applications*, Springer International Publishing, 2019, pp. 15–35. DOI: 10.1007/978-3-030-15887-3_2.

[10] L. A. Maghrabi, M. Altwijri, S. S. Binyamin, F. S. Alallah, D. Hamed, and M. Ragab, "Secure biometric identification using orca predators algorithm with deep learning: Retinal iris image analysis," *IEEE Access*, vol. 12, pp. 18 858–18 867, 2024. DOI: 10.1109/ACCESS.2024.3360871.

[11] P. Padm and S. D. Srinivasan, "A survey on biometric based authentication in cloud," in *IEEE*, Jan. 2017.

[12] A. M. Q. Musleh and A. M. O. Al-Azzani, "Developing a model for offline signature verification using cnn architectures and genetic algorithm," *Sana'a Univ. J. Appl. Sci. Technol.*, vol. 1, no. 3, Sep. 2023. DOI: 10.59628/jast.v1i3.314.

[13] Z. Rui and Z. Yan, "A survey on biometric authentication: Toward secure and privacy-preserving identification," 2019. DOI: 10.1109/ACCESS.2018.2889996.

[14] R. Ryu, S. Yeom, D. Herbert, and J. Dermoudy, "The design and evaluation of adaptive biometric authentication systems: Current status, challenges and future direction," Dec. 2023. DOI: 10.1016/j.icte.2023.04.003.

[15] National Science and Technology Council, *Iris Recognition*. 2019.

[16] C. Raghavendra, A. K. Dean, C. S. Sivasubramanian, and H. Cse, "Iris technology: A review on iris based biometric systems for unique human identification," 2017. DOI: 10.1109/ICAMMAET.2017.8186679.

[17] Dr Graham Furness, *Https://insighteye.com.au/iris-recognition-ready-to-take-over/*.

[18] S. Marĉelja, "Mathematical description of the responses of simple cortical cells," *J Opt Soc Am*, 1980.

[19] R. Mehrotra, K. R. Namuduri, and N. Ranganathan, "Gabor filter-based edge detection," 1992.

[20] K. Ashwini, G. N. K. Murthy, S. Raviraja, and G. A. Srinidhi, "A novel multimodal biometric person authentication system based on ecg and iris data," *Biomed Res Int*, vol. 2024, p. 8 112 209, 2024. DOI: 10.1155/2024/8112209.

[21] D. Harikrishnan, N. Sunilkumar, J. Shelby, N. Kishor, and G. Remya, "An effective authentication scheme for a secured iris recognition system based on a novel encoding technique," *Meas. Sensors*, vol. 25, Feb. 2023. DOI: 10.1016/j.measen.2022.100626.

[22] T. Sueishi, A. Jingu, S. Yachida, M. Inoue, Y. Ogino, and M. Ishikawa, "Dynamic iris authentication by high-speed gaze and focus control," in *2021 IEEE/SICE International Symposium on System Integration (SII 2021)*, Institute of Electrical and Electronics Engineers Inc., Jan. 2021, pp. 813–814. DOI: 10.1109/IEEECONF49454.2021.9382650.

[23] H. Hafeez, M. N. Zafar, C. A. Abbas, H. Elahi, and M. O. Ali, "Real-time human authentication system based on iris recognition," *Eng*, vol. 3, no. 4, pp. 693–708, Dec. 2022. DOI: 10.3390/eng3040047.

[24] L. Attard, C. J. Debono, G. Valentino, and M. D. Castro, "Tunnel inspection using photogrammetric techniques and image processing: A review," Oct. 2018. DOI: 10.1016/j.isprsjprs.2018.07.010.

[25] M. Abdalla, P.-A. Fouque, and D. Pointcheval, "Lncs 3386 - password-based authenticated key exchange in the three-party setting," [Online]. Available: http://www.di.ens.fr/users/mabdalla,fouque,pointche, 2005.

[26] K. Sireesha and P. Amaravathi, "Ror model based formal security analysis and informal security analysis," 2021.